

# Copper ATRP Catalysts with Quadridentate Amine Ligands: The Effects of Steric and Electronic Tuning on the Polymerization of Methyl Methacrylate

Robert M. Johnson, Christina Ng, Claire C. M. Samson, and Cassandra L. Fraser\*

Department of Chemistry, University of Virginia, McCormick Road, P.O. Box 400319, Charlottesville, Virginia 22904-4319

Received July 20, 1999; Revised Manuscript Received August 28, 2000

**ABSTRACT:** A series of nine linear quadridentate ligands with amine, pyridine, and quinoline donor groups of different steric and electronic demand were prepared for complexation with CuX and CuX<sub>2</sub> halide salts. Select Cu(II) complexes were reacted with either AgPF<sub>6</sub> or NaBPh<sub>4</sub> to generate dicationic di-PF<sub>6</sub> salts and monocationic halo-BPh<sub>4</sub> complexes, respectively. These Cu complexes with different oxidation states, counterions, and chelate ligands were screened as catalysts for the atom transfer radical polymerization (ATRP) of methyl methacrylate (MMA) in toluene or anisole solution at 80 °C. Catalysts were generated in situ or were isolated prior to subsequent introduction to the reaction media. Copper metal was added to all polymerizations of precomplexed catalyst systems (i.e., all Cu(II) complexes and those prepared ahead of time from CuBr). Molecular weight vs percent monomer conversion and kinetics plots are provided to illustrate the level of control that was achieved under various conditions. PDIs of poly(methyl methacrylate) (PMMA) products were generally low (~1.1–1.4). Reaction rates exhibited the following trend: [Cu(ligand)X]BPh<sub>4</sub> > Cu(ligand)X > Cu(ligand)X<sub>2</sub>, with the last of these showing longer induction periods. In general, reactions were faster and more controlled in anisole than in toluene. Polymerizations were slower with catalysts made from ligands bearing fluorine substituents than with nonfluorinated analogues. Other Cu systems with bulky quinoline or methylpyridine groups in the terminal positions tended to exhibit poor reactivity and/or molecular weight control. Consistent with the accepted mechanism of ATRP, analysis of tacticity indicates no special stereoselectivity was observed in polymerizations run with catalysts bearing chiral quadridentate ligands.

## Introduction

Atom transfer radical polymerization (ATRP) has allowed for significant advances in control over molecular weights and architectures in macromolecular synthesis.<sup>1</sup> Numerous styrene and acrylate monomers have been polymerized using transition metal catalysts in conjunction with alkyl or sulfonyl halide initiators.<sup>2,3</sup> It is assumed that the metal is involved in reversible halide abstraction from the initiating and propagating species, generating small quantities of radicals at equilibrium and a formally oxidized metal halide species. Metal complexes that are capable of interconverting between oxidation states differing by one unit with concomitant changes in coordination number are frequently employed. These include Cu(I) to Cu(II)X, Ni(II) to Ni(III)X, or Ru(II) to Ru(III)X, among other metal systems. The field of ATRP catalyst development is growing rapidly, and numerous systems have been described. Those that have been investigated most thoroughly to date tend to fall into two general categories: (1) metal phosphine and organometallic compounds based on Ru,<sup>4</sup> Rh,<sup>5</sup> Fe,<sup>6</sup> Ni,<sup>7,8</sup> and Re,<sup>9</sup> which have been explored in detail by the research groups of Sawamoto and Jérôme; or (2) traditional coordination compounds, most commonly based on copper. Complexes with bipyridine<sup>10–12</sup> and chelating amines<sup>13–15</sup> have been pioneered by Matyjaszewski, whereas pyridyl-methanimine<sup>16,17</sup> chelates have been studied by Haddleton and co-workers.

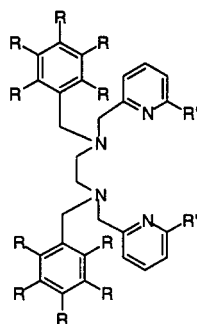
Though much has been accomplished with known ATRP catalysts, very few of these lend themselves to convenient, systematic tuning of the steric and electronic environment around the metal center. Examples

of systems that have been varied most extensively to date include copper bpy catalysts. These have been modified with substituents on the bpy ligand, in large part to improve catalyst solubility in nonpolar reaction media.<sup>10,18</sup> A variety of copper salts have also been explored. Anions of different donor strengths include halides,<sup>10,19</sup> triflates,<sup>20</sup> and carboxylates,<sup>21</sup> as well as noncoordinating counterions such as hexafluorophosphate, PF<sub>6</sub><sup>–</sup>.<sup>22</sup> Since pyridylimine ligands are conveniently prepared from carbonyl compounds and amines by Schiff base condensation, the generation of numerous derivatives of Cu(I) complexes of this ligand set has also been straightforward.<sup>16,17</sup> The optimization of ATRP reactions using copper in conjunction with a plethora of chelating amine ligands is also under investigation.<sup>18</sup>

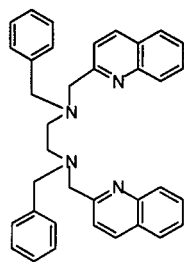
Recently, we undertook the synthesis of a series of linear quadridentate ligands bearing pyridine or quinoline donors and both chiral and achiral diamine groups. Complexation of these ligands to many first-row metal ions (M(II) = Mn, Fe, Co, Ni, Cu, Zn; M(III) = Fe, Co) has also been investigated.<sup>23</sup> Since all three components of these ligands may be readily varied—the diamine backbone, the terminal donor groups, as well as the nonchelating alkyl groups on the tertiary nitrogen centers—we have suggested that these systems could be ideal for investigations of the influence of steric and electronic factors on a wide variety of catalytic reactions, in both small molecule and polymer synthesis.<sup>23</sup> Since these quadridentate chelates are hybrids of known amine and pyridine ligands commonly used in controlled polymerization reactions, it was of interest to us to employ copper complexes of this series as ATRP catalysts. The versatility of picolylamine chelates and their

amenability to systematic tuning has also recently been appreciated by Matyjaszewski and co-workers.<sup>15,18</sup> Preliminary studies described herein were concerned with the influence of catalyst preparation, copper halide salts of different oxidation states including some with non-coordinating counterions, and variations in electronic and steric features of the ligand on the polymerization of methyl methacrylate (MMA) in toluene and anisole solution at 80 °C.

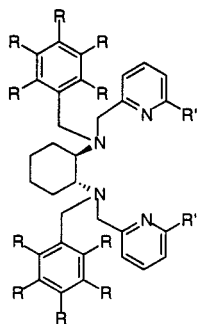
**Ligand Preparation.** A series of linear quadridentate ligands (**1–9**) was prepared to assess the effect of steric and electronic factors on catalyst reactivity. These ligands are comprised of consecutive five-membered metallocycle rings. It has been noted that this ring size is optimal for achieving control in copper-catalyzed ATRP reactions.<sup>18</sup> Bulky quinoline (qn) and methylpyridine (pyMe) containing ligands were prepared for comparison with those bearing pyridine (py) groups. The reactivities of catalysts made from ethylenediamine (en) backbone ligands are contrasted with those generated from bulkier *R,R*-cyclohexanediamine (*R,R*-cn) ones. Moreover, ligands were alkylated with benzyl (Bn) groups as well as a fluorinated benzyl analogue (F<sub>5</sub>Bn) in order to explore the effect of subtle electronic differences on reactivity. These variations are expected to be reflected in the reaction kinetics since ATRP reactions tend to be sensitive to catalyst oxidation potentials—the signature of the electron richness of the metal center.<sup>18,20,25</sup> Moreover, steric factors influence the accessibility of the initiator and propagating species to the metal center.<sup>16,18,20,26</sup> Ligands are designated in the following manner: the internal diamine (en or *R,R*-cn) is indicated first, followed by the noncoordinating benzyl group (Bn or F<sub>5</sub>Bn) in parentheses, and then the terminal donor groups (py, qn, or pyMe).



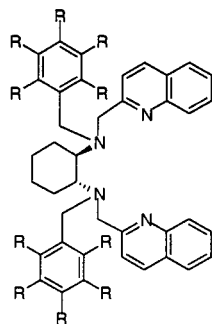
- 1 R, R' = H; en(Bn)py  
2 R = F, R' = H; en(F<sub>5</sub>Bn)py  
3 R = H, R' = Me; en(Bn)pyMe



4 en(Bn)qn



- 5 R, R' = H; *R,R*-cn(Bn)py  
6 R = F, R' = H; *R,R*-cn(F<sub>5</sub>Bn)py  
7 R = H, R' = Me; *R,R*-cn(Bn)pyMe



- 8 R = H; *R,R*-cn(Bn)qn  
9 R = F; *R,R*-cn(F<sub>5</sub>Bn)qn

The quadridentate ligands **1–9** were formed in three easy steps by previously described methods.<sup>23,24</sup> Schiff base condensation between a diamine (or a diammonium salt in the presence of a base) and a pyridyl or quinoline aldehyde was followed by reduction of the resulting imine with sodium borohydride in methanol solution. Subsequent alkylation of the internal secondary amine nitrogen was accomplished by deprotonation with NaH, followed by reaction with various alkyl halides.<sup>27</sup> Quadridentate ligands were purified by flash column chromatography on silica gel or, in some cases, by recrystallization.

Originally, these quadridentate ligands were designed to adopt *C*<sub>2</sub> symmetric cis  $\alpha$  topologies upon chelation to octahedral metal centers, with chiral variants likely to form single diastereomers.<sup>23</sup> The “zigzag” shape of cis  $\alpha$  complexes is analogous to that of many ansa metallocenes. The potential of this ligand design for olefin polymerization catalysts has also been recognized by Rieger et al.<sup>28</sup> It is not anticipated, however, that topological or stereochemical control will be achieved upon complexation of chiral ligands to copper centers for the following reasons. Copper(II) complexes are noted for their “plasticity”,<sup>29</sup> that is, their tendency to alternate between four-, five-, or six-coordinate geometries in response to even quite subtle changes in the ligand set, solvent conditions, or reaction medium. It is also not uncommon for several species of different coordination number to be present at once in solution.<sup>30</sup> There exists considerable precedent for this kind of structural variation with quadridentate picolylamine systems.<sup>31</sup> Furthermore, it is not uncommon for complexes with the Cu(I) oxidation state to adopt two-, three-, and four-coordinate structures. However, since complexes that are five-coordinate and higher are rare, six-coordinate cis  $\alpha$  topologies are unlikely.<sup>35</sup> Moreover, the widely accepted mechanism for ATRP, wherein the catalyst abstracts a halide from RX, and monomer reacts with the resulting radical, R<sup>•</sup>, outside the coordination sphere of the metal, seems to preclude stereocontrolled polymerization of simple monomers through the use of chiral ATRP catalysts.<sup>36</sup> The tacticity of certain PMMA products was examined nonetheless, to further verify that this is the case.

**Synthesis of Copper Catalysts.** There are many ways of generating active ATRP catalysts using nitrogen ligands, copper salts, and additives. Most commonly, catalysts are prepared by the reaction of ligands with copper salts in situ, in the presence of monomer. Copper halides are used most frequently,<sup>10–19</sup> although other salts have also been employed.<sup>20–22</sup> The Cu(I) halides are typically purified prior to their inclusion in the reaction mixture. However, commercial CuX reagents can also be used as received, since the presence of Cu(II) impurities actually improves control during the establishment of equilibrium in the initial stages of the ATRP reaction.<sup>21,22</sup> This has been proven through the intentional introduction of varying amounts of Cu(II) salts to Cu(I)X-catalyzed reactions.<sup>21</sup> It has also been shown that reactions may be run in the presence of oxygen as long as small amounts of Cu(0) are added to the reaction mixture. Any Cu(II) that is generated by air oxidation is thus reduced to the active Cu(I) catalyst by copper metal.<sup>37</sup> Similarly, more stable Cu(II) salts may be used in place of Cu(I) species if sufficient Cu(0) is present in the reaction medium to generate the Cu(I) catalyst by a redox reaction.<sup>20</sup> These findings were

**Table 1. Electronic Absorption Spectral Data (190–1100 nm) for Precomplexed Catalyst Systems in Methylene Chloride**

catalyst	description	wavelength (nm) <sup>a</sup>
Cu{en(Bn)py}Br <sup>b</sup>	pale green powder	228 (7870), 262 (8250), 299 sh, 757 (287)
Cu{en(Bn)py}Br <sub>2</sub>	pale blue-green solid	262 (14 000), 301 sh, 774 (310)
Cu{en(F <sub>5</sub> Bn)py}Br <sup>c</sup>	pale green powder	232 (10 000), 260 (12 000), 320 sh, 780 (140)
Cu{en(Bn)pyMe}Br <sup>b</sup>	pale green powder	229 (10 600), 263 (11 000), 335 (3420), 710 (54)
Cu{en(Bn)qn}Br <sup>b</sup>	orange powder	236 (52 000), 318 (9400), 750 (190)
[Cu{en(Bn)py}Cl](BPh <sub>4</sub> )	green needles	236 (24 000), 259 sh, 299 sh, 771 (270)
[Cu{en(Bn)py}Br](BPh <sub>4</sub> )	green needles	231 (34 000), 260 sh, 276 sh, 291 sh, 779 (130)
[Cu{en(Bn)py}](PF <sub>6</sub> ) <sub>2</sub>	blue-violet needles	262 (9600), 288 (4300), 642 (850)
Cu{ <i>R,R</i> -cn(Bn)py}Br <sup>b</sup>	yellow-green powder	229 (10 400), 261 (6640), 294 (5140), 358 (2380), 730 (35)
Cu{ <i>R,R</i> -cn(Bn)py}Br <sub>2</sub>	green solid	229 (8700), 262 (6900), 314 (3990), 728 (201)
Cu{ <i>R,R</i> -cn(F <sub>5</sub> Bn)py}Br <sup>b</sup>	green powder	230 (10 000), 261 (7600), 286 (5400), 346 (2600), 764 (52)
Cu{ <i>R,R</i> -cn(Bn)pyMe}Br <sup>b</sup>	pale yellow-green powder	229 (10 000), 265 (9000), 350 (2900)
Cu{ <i>R,R</i> -cn(Bn)qn}Br <sup>b</sup>	orange powder	237 (26 000), 289 (6900), 322 (6500), 410 (2100)
[Cu{ <i>R,R</i> -cn(F <sub>5</sub> Bn)qn}][Br] <sup>d</sup>	yellow powder	241 (30 000), 281 sh, 316 (10 000), 322 (10 000), 394 (2400)
Cu{ <i>R,R</i> -cn(F <sub>5</sub> Bn)py}Cl](BPh <sub>4</sub> )	yellow-green powder	235 (26 000), 260 sh, 289 sh, 740 (130)
[Cu{ <i>R,R</i> -cn(F <sub>5</sub> Bn)py}](PF <sub>6</sub> ) <sub>2</sub> <sup>c</sup>	blue microcrystalline solid	262 (13 000), 294 (6000), 584 (250)

<sup>a</sup> Extinction coefficients (M<sup>-1</sup> cm<sup>-1</sup>) are given in parentheses. sh = shoulder. <sup>b</sup> Catalyst systems formed from CuBr and indicated ligand in air may be mixtures of Cu(I) and Cu(II) species. <sup>c</sup> Range: 190–820 nm. <sup>d</sup> No evidence of paramagnetic Cu(II) species.

taken into account in the preparation of Cu complexes of ligands **1–9** for screening as catalysts for the atom transfer radical polymerization of MMA.

A variety of different catalyst preparation conditions were explored. Ligands were combined with CuBr to generate catalysts in situ, and for en(Bn)py **1**, reactions were run with both purified and unpurified CuX for comparison. It was also of interest to see what effect it might have on ATRP reactivity if CuX and CuX<sub>2</sub> salts were reacted with ligands, and the resulting complexes were isolated and purified as solids prior to submission to the reaction media for catalyst screening. Reaction of Cu(I) halides with ligands under inert atmosphere could lead to copper(I) quadridentate products. However, since the presence of Cu(II) species in the reaction media enhances control, we reasoned that any oxidation of Cu(I) products to Cu(II) during catalyst synthesis might be addressed through the introduction of Cu(0) into the polymerization reaction media. Thus, a much more convenient approach was taken. Commercial CuX salts were used as received and were combined with the appropriate ligand in ethanol. For certain ligand–metal combinations, quinoline-containing ligands in particular, solutions were refluxed to facilitate dissolution. Reaction solutions were concentrated, and the resulting residues were typically recrystallized from CH<sub>2</sub>Cl<sub>2</sub>/Et<sub>2</sub>O.

For ligands with pyridyl donor groups (**1–3** and **5–7**), green solutions resulted upon reaction with Cu(I) salts in ethanol. Solids that are pale green in color, indicative of the presence of Cu(II), were isolated after precipitation of the complexes from CH<sub>2</sub>Cl<sub>2</sub>/Et<sub>2</sub>O. Since complexes are likely to be mixtures of Cu(I) and Cu(II) species, this precluded characterization of the catalysts as unique products. Nonetheless, <sup>1</sup>H NMR spectra were recorded and broad signals were observed, indicating the presence of paramagnetic d<sup>9</sup> Cu(II). Electronic absorption spectral data for precomplexed copper catalyst systems in CH<sub>2</sub>Cl<sub>2</sub> solution are provided in Table 1. Molar conductivity measurements of 1 mM acetonitrile solutions reveal that, on average, complexes are 1:1 electrolytes ( $\Lambda_M = 69\text{--}99 \text{ } \Omega^{-1} \text{ mol}^{-1} \text{ cm}^2$ ). That is, complexes may be formulated as monocationic [Cu(ligand)]X or possibly [Cu(ligand)X]X species, with halide counterions in the outer sphere. Solvent complexes, [Cu(ligand)(solvent)]X and [Cu(ligand)(solvent)X]X, would also be consistent with the observed conductivity data. In contrast, the bulkier quinoline-containing ligands **4**, **8**, and **9** produced yellow or

orange-yellow complexes upon combination with Cu(I) salts. <sup>1</sup>H NMR analysis of the product obtained upon reaction of CuX with **9** indicated a diamagnetic d<sup>10</sup> Cu(I) species. There was no evidence of signal broadening attributable to Cu(II) byproducts. These data suggest that bulkier ligands better stabilize the lower Cu(I) oxidation state. This might be rationalized in the following manner. Steric interactions between terminal quinoline groups prevent the adoption of the planar copper coordination geometry favored by Cu(II).<sup>38</sup> Nonplanar, tetrahedral ligand environments are more ideally suited for Cu(I) species.<sup>35</sup> Moreover, steric bulk around the metal center could destabilize or even prevent halide ligand coordination, again favoring the lower oxidation state for copper.

There is considerable precedent for Cu(II) complexes of these and related Cu(II) picolylamine ligands.<sup>31–34</sup> For this study, complexes of cupric halides were prepared in ethanol using the appropriate CuX<sub>2</sub> salt, followed by precipitation from CH<sub>2</sub>Cl<sub>2</sub>/Et<sub>2</sub>O, analogous to Cu(I) complexes. Again, ligands react with CuX<sub>2</sub> salts immediately upon mixing. These d<sup>9</sup> Cu(II) systems are paramagnetic and are typically 1:1 electrolytes in acetonitrile solution ( $\Lambda_M = 110\text{--}116 \text{ } \Omega^{-1} \text{ mol}^{-1} \text{ cm}^2$ ). Depending on the specific halide counterion and the steric bulk of the ligand, green, teal, or blue solutions are commonly generated.<sup>18,24,31–34</sup> This is consistent with five- and six-coordinate structures and with what has been previously observed for these systems in the solid state via X-ray crystallographic analysis.<sup>18,31</sup> As expected, differences in the electronic absorption spectra of Cu(II) complexes correlate with structural and electronic variations. Complexes of the fluorinated ligand **2** display an absorption band in the visible region ( $\lambda_{\text{max}} = 780 \text{ nm}$ ) at a lower energy than for the complex of the analogous nonfluorinated analogue **1** ( $\lambda_{\text{max}} = 757 \text{ nm}$ ). A similar observation was made for the complexes of the *R,R*-cn backbone ligands **5** and **6** [Cu{*R,R*-cn(Bn)py}Br:  $\lambda_{\text{max}} = 730 \text{ nm}$ ; Cu{*R,R*-cn(F<sub>5</sub>Bn)py}Br:  $\lambda_{\text{max}} = 764 \text{ nm}$ ]. Thus, decreased chelate donor strength correlates with lower energy UV/vis bands. It should also be noted that complexes with the more substituted *R,R*-cn backbone ligands possess higher energy d–d transitions than those bearing ethylenediamine (en) donors.

More reactive ATRP catalysts have been generated through the replacement of cuprous halides, CuX, with copper salts that contain a more loosely associated



triflate ligand,  $\text{CuOTf}$ ,<sup>20</sup> or a noncoordinating hexafluorophosphate counterion,  $\text{CuPF}_6$ .<sup>22</sup> Thus, it was also of interest to prepare Cu(II) quadridentates with noncoordinating counterions. Di- $\text{PF}_6$  salts,  $[\text{Cu}(\text{ligand})](\text{PF}_6)_2$ , of ligands **1** and **6** were generated by combining acetonitrile solutions of  $[\text{Cu}(\text{ligand})\text{Cl}_2]$  with  $\text{AgPF}_6$ . The green solutions turned blue upon mixing, with concomitant precipitation of  $\text{AgCl}$ . Purification from  $\text{CH}_2\text{Cl}_2/\text{MeOH}$  yielded blue solids that are 2:1 electrolytes ( $\Lambda_M = 218\text{--}236 \Omega^{-1} \text{mol}^{-1} \text{cm}^2$ ). Consistent with the color changes observed, lower coordinate Cu(II) hexafluorophosphate complexes of ligands **1** and **6** show higher energy d–d absorption bands in UV/vis spectra than the higher coordinate Cu(II) precursors. X-ray crystallographic analysis of a related hexafluoroantimonate complex of ligand **6**,  $[\text{Cu}\{R,R\text{-}cn(\text{F}_5\text{Bn})\text{py}\}](\text{SbF}_6)_2$ , indicated a four-coordinate square-planar structure in the solid state.<sup>24</sup> Since dicationic di- $\text{PF}_6$  species could exhibit limited solubilities in typical ATRP reaction media, tetraphenyl borate salts were also prepared. Reaction of the Cu complexes  $[\text{Cu}\{\text{en}(\text{Bn})\text{py}\}\text{Cl}_2]$ ,  $[\text{Cu}\{\text{en}(\text{Bn})\text{py}\}\text{Br}_2]$ , and  $[\text{Cu}\{R,R\text{-}cn(\text{F}_5\text{Bn})\text{py}\}\text{Cl}_2]$  with  $\text{NaBPh}_4$  in  $\text{CH}_3\text{CN}$  generated blue solutions. After workup and purification by recrystallization from  $\text{CH}_2\text{Cl}_2/\text{MeOH}$ , green needles were obtained. These complexes are ~1:1 electrolytes ( $\text{CH}_3\text{CN}$ ) ( $\Lambda_M = 79\text{--}96 \Omega^{-1} \text{mol}^{-1} \text{cm}^2$ ), which suggests a  $[\text{Cu}(\text{ligand})\text{X}]\text{BPh}_4$  formulation, and the replacement of only one of the original halides by a noncoordinating  $\text{BPh}_4^-$ . Attempts were made to replace both halides and to prepare the dication,  $[\text{Cu}\{\text{en}(\text{Bn})\text{py}\}](\text{BPh}_4)_2$ , using  $\text{AgBPh}_4$ .<sup>39</sup> However, the poor solubility of  $\text{AgBPh}_4$  in common polar and nonpolar organic solvents, combined with its instability, precluded the synthesis of the dicationic Cu(II) complex by this route.

Cu complexes of ligands **1–9** were investigated by cyclic voltammetry. Unfortunately, only multiple, irreversible processes were evident in the voltammograms. Fluorination of the quadridentate ligand and for other metal complexes of this ligand series, namely Mn(II), Co(II), and Fe(II), resulted in the expected increase in metal oxidation potential relative to unfluorinated parent compounds. For example,  $\text{Fe}\{\text{en}(\text{Bn})\text{py}\}\text{Cl}_2$  and  $\text{Fe}\{\text{en}(\text{F}_5\text{Bn})\text{py}\}\text{Cl}_2$  show a difference of 80 mV in their oxidation potentials, which provides an estimate of the electronic differences that might be expected as a result of ligand fluorination.<sup>18</sup>

**Polymerization Reactions.** The polymerization of methyl methacrylate was performed at 80 °C in either toluene or anisole solution using ethyl 2-bromoisobutyrate as the initiator. Before carrying out systematic studies on the effect of electronic and steric factors of copper quadridentates on reactivity and molecular weight control, it was important to determine what was necessary in terms of monomer purification, catalyst preparation, and other general reaction conditions. Haddleton and co-workers have shown that copper imine catalysts work well even when MMA is not purified. In some cases, inhibitors in commercial MMA actually enhanced reaction rates.<sup>40</sup> Moreover, it has been demonstrated that it is possible to run reactions in air if Cu(0) is added to the reaction mixtures. Yet, reactions run under an ambient atmosphere in toluene solution using precomplexed  $\text{Cu}\{R,R\text{-}cn(\text{Bn})\text{py}\}\text{Br}$  and unpurified monomer produced polymers with high PDIs (~1.3–3.3). In many cases, multimodal GPC traces were observed. Hence, all subsequent reactions were run under a nitrogen atmosphere using monomer that had

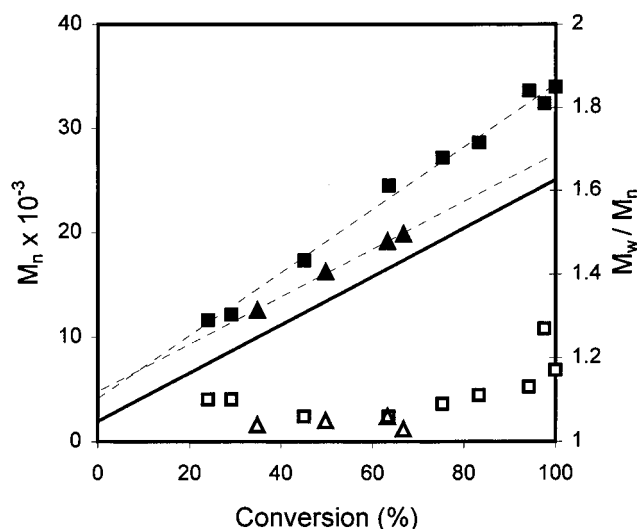


**Figure 1.** Comparison of  $M_n$  vs percent monomer conversion plots for MMA polymerizations in anisole at 80 °C promoted by en backbone catalysts of different oxidation states,  $\text{Cu}\{\text{en}(\text{Bn})\text{py}\}\text{Br}$  (in situ) (■) and  $\text{Cu}\{\text{en}(\text{Bn})\text{py}\}\text{Br}_2$  (precomplexed) (▲). (— =  $M_n(\text{calcd})$ ; corresponding open symbols represent PDIs).

been purified by passage through basic alumina or distillation from  $\text{CaH}_2$ . Generally, new conditions were tested for the parent complexes of  $\text{en}(\text{Bn})\text{py}$ , **1**, and/or  $R,R\text{-}cn(\text{Bn})\text{py}$ , **5**, before complexes of other ligands of different steric and electronic demand were screened. Reactions were run using catalysts that were generated in situ, as well as with catalysts that were prepared and isolated prior to use in polymerizations. For catalysts formed in situ, greater reaction rates and molecular weight control were observed for CuBr:quadridentate ratios of 1:1.5 as compared with reactions run with 1:1.1 ratios. And in the absence of Cu(0), reactions run with ligands **1** or **5** that were precomplexed with CuBr showed negligible reactivity.<sup>41,42</sup> Thus, Cu(0) was added to all subsequent runs (for catalysts prepared from Cu(I) salts:  $\text{Cu}(0)/\text{Cu}(\text{I}) = 0.1:1$ ; for catalysts prepared from Cu(II) salts:  $\text{Cu}(0)/\text{Cu}(\text{II}) = 1:1$ ).

To investigate the effect of catalyst electronics on MMA polymerization, Cu complexes with different oxidation states, complexes with coordinating and noncoordinating counterions, and other sets bearing ligands with and without electron-withdrawing fluorine groups were compared. Copper(I) catalysts generated in situ from CuBr and quadridentates and certain precomplexed Cu(I) and Cu(II) systems with added Cu(0) are viable catalysts for MMA polymerization. For example,  $M_n$  vs percent monomer conversion plots for Cu(I) and Cu(II)  $\text{en}(\text{Bn})\text{py}$ , **1**, reactions run in anisole (Figure 1) and in toluene (Figure 2) are essentially linear, which is one measure of the degree of control for a polymerization. However, measured molecular weights are higher than calculated values, indicative of the loss of some competent initiator species in the early stages of the reaction during the establishment of equilibrium or of poor initiation. Reactions of in situ catalysts in anisole show slightly better control than do preformed ones in toluene, as indicated by lower PDIs and a better match with calculated molecular weights based on monomer-to-initiator ratios,  $[\text{M}]_0/[\text{I}]_0$ . In toluene, reactions using catalysts prepared from Cu(I) tend to be slightly more controlled than those run with Cu(II) species, but they are comparable in anisole, as is indicated by the PDIs of polymer products (Figures 1 and 2).

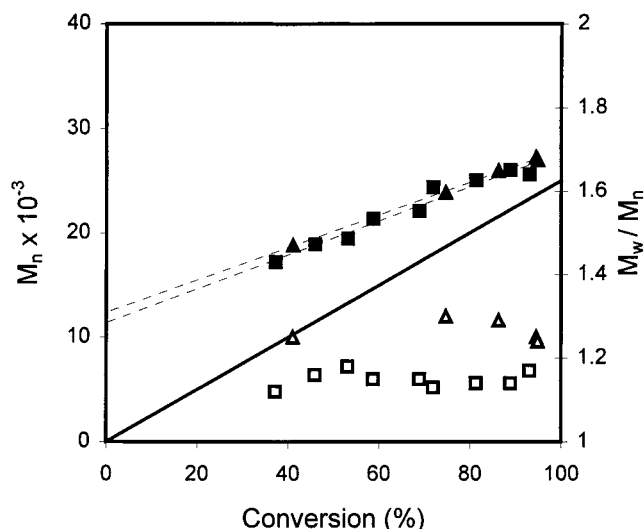


**Figure 2.** Comparison of  $M_n$  vs percent monomer conversion plots for MMA polymerizations in toluene at 80 °C promoted by precomplexed en backbone catalysts of different oxidation states,  $\text{Cu}\{\text{en}(\text{Bn})\text{py}\}\text{Br}$  (■) and  $\text{Cu}\{\text{en}(\text{Bn})\text{py}\}\text{Br}_2$  (▲). (— =  $M_n(\text{calcd})$ ; corresponding open symbols represent PDIs).

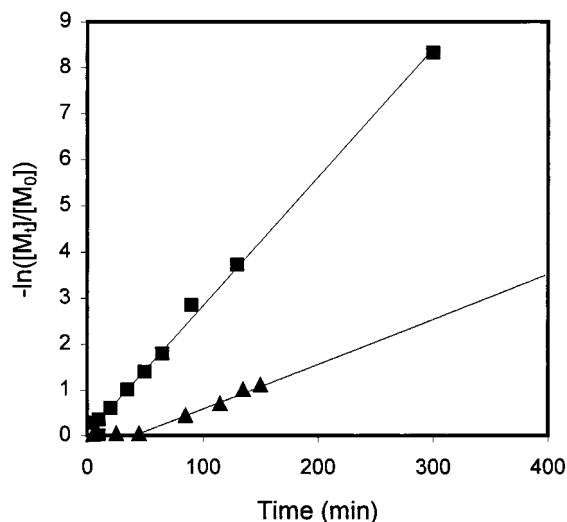


**Figure 3.** Kinetics plots for the polymerization of MMA in anisole at 80 °C using  $\text{Cu}\{\text{en}(\text{Bn})\text{py}\}\text{Br}$  (in situ) (■) and  $\text{Cu}\{\text{en}(\text{Bn})\text{py}\}\text{Br}_2$  (▲) catalysts.

Kinetics plots reveal that reactions are faster and generally more controlled in anisole as compared with toluene. For example, in anisole, kinetics plots are first-order with respect to monomer for  $\text{Cu}\{\text{en}(\text{Bn})\text{py}\}\text{Br}$  generated in situ ( $k_{\text{obs}} = 0.028 \text{ min}^{-1}$ ) and for the  $\text{Cu}(\text{II})$  catalyst ( $k_{\text{obs}} = 0.011 \text{ min}^{-1}$ ) (Figure 3). In toluene, reactions with the  $\text{Cu}(\text{I})/1$  precomplexed catalyst show some S-shaped curvature in the kinetics plot ( $k_{\text{obs}} = 0.007 \text{ min}^{-1}$ , estimated from linear regression of data), whereas those with the  $\text{Cu}(\text{II})$  catalyst ( $k_{\text{obs}} = 0.012 \text{ min}^{-1}$ ) have comparable rates but longer induction periods as compared with anisole reactions (toluene, ~150 min; anisole, ~45 min) (Figure 4). Induction periods have been observed for other ATRP catalysts and have been attributed to the establishment of equilibrium (i.e., reduction of  $\text{Cu}(\text{II})$  to  $\text{Cu}(\text{I})$  by  $\text{Cu}(\text{0})$  before ATRP may proceed) or the consumption of residual oxygen.<sup>8,16,36,37,41</sup> Results obtained using ligand **5**, *R,R*-*c*n(Bn)py, are similar to those for en backbone systems. Again, precomplexed  $\text{Cu}(\text{I})/\text{Cu}(\text{0})$  systems show faster reaction rates ( $k_{\text{obs}} = 0.10 \text{ min}^{-1}$ ), and polymers

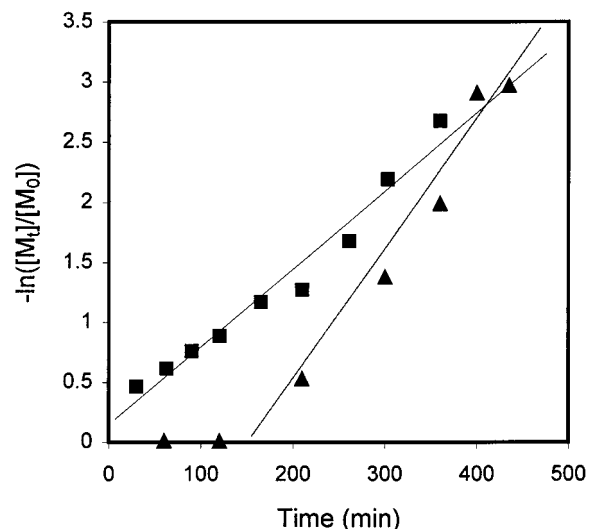


**Figure 4.** Kinetics plots for the polymerization of MMA in toluene at 80 °C using precomplexed  $\text{Cu}\{\text{en}(\text{Bn})\text{py}\}\text{Br}$  (■) and  $\text{Cu}\{\text{en}(\text{Bn})\text{py}\}\text{Br}_2$  (▲) catalysts.

exhibited slightly narrower molecular weight distributions as compared with those formed from  $\text{Cu}(\text{II})/\text{Cu}(\text{0})$  catalysts ( $k_{\text{obs}} = 0.003 \text{ min}^{-1}$ ) in toluene solutions.

Noncoordinating counterions were also explored with these Cu quadridentate systems. Hexafluorophosphate salts,  $[\text{Cu}(\text{ligand})](\text{PF}_6)_2$ , of **1** and **6** were nearly insoluble in the MMA/toluene reaction medium, and negligible reactivity<sup>41</sup> was observed even after 10 h. In anisole, the reactions remained colorless for ~45 min, after which time a blue color developed. The kinetics plot confirms a ~30 min induction period followed by a very slow rate of polymerization ( $k_{\text{obs}} = 0.0033 \text{ min}^{-1}$ ). Inspection of the  $M_n$  vs percent monomer conversion plot reveals, however, that polymerizations using this catalyst system are uncontrolled, as is also evidenced by multimodal GPC traces and high PDIs (~1.3–2.2).

More promising results were obtained with tetraphenyl borate salts.<sup>43</sup> Polymerizations utilizing  $[\text{Cu}\{\text{en}(\text{Bn})\text{py}\}\text{Br}](\text{BPh}_4)$  resulted in accelerated reaction rates relative to both  $\text{Cu}\{\text{en}(\text{Bn})\text{py}\}\text{Br}$  and  $\text{Cu}\{\text{en}(\text{Bn})\text{py}\}\text{Br}_2$  in both solvent systems. Anisole reactions exhibited a short induction period (~5 min) and were essentially complete after ~1.5 h ( $k_{\text{obs}} = 0.039 \text{ min}^{-1}$ ). Linear kinetics plots correlate with a constant number of propagating species throughout the course of the reaction (Figure 5). Corresponding  $M_n$  vs percent monomer conversion plots are also linear for  $[\text{Cu}\{\text{en}(\text{Bn})\text{py}\}\text{Br}](\text{BPh}_4)$  (Figure 6), though there is evidence of poor initiation in anisole and in toluene. Although molecular weight distributions remain relatively narrow (<1.3) up to ~75% conversion for reactions with Br catalysts in either solvent, they broaden significantly (~1.5–1.75) beyond this point. Analogous to what has been observed for Cu bipyridine catalysts with noncoordinating counterions, increased rates are accompanied by some loss of molecular weight control as compared with the parent  $\text{Cu}(\text{I})\text{Br}$  and  $\text{Cu}(\text{II})\text{Br}_2$  systems.<sup>20,22</sup>

Previously, it has been reported that halide exchange between chloride catalysts and bromide initiators can improve the molecular weight control in ATRP reactions by helping to ensure that initiation is fast relative to propagation.<sup>19</sup> Polymerizations using a chloride catalyst,  $[\text{Cu}\{\text{en}(\text{Bn})\text{py}\}\text{Cl}](\text{BPh}_4)$ , in anisole and toluene reached ~90% conversion in ~1.5 h ( $k_{\text{obs}} = 0.025 \text{ min}^{-1}$ ) and ~4 h ( $k_{\text{obs}} = 0.006 \text{ min}^{-1}$ ), respectively. Thus, rates are

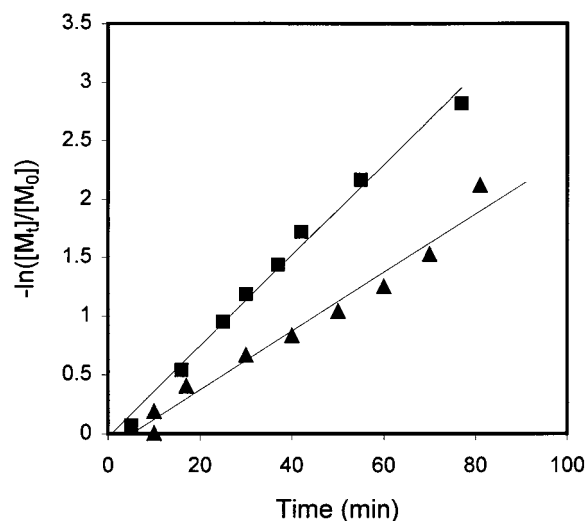


**Figure 5.** Kinetics plots for the polymerization of MMA in anisole at 80 °C catalyzed by  $[\text{Cu}\{\text{en}(\text{Bn})\text{py}\}\text{Br}]\text{BPh}_4$  (■) and  $[\text{Cu}\{\text{en}(\text{Bn})\text{py}\}\text{Cl}]\text{BPh}_4$  (▲).

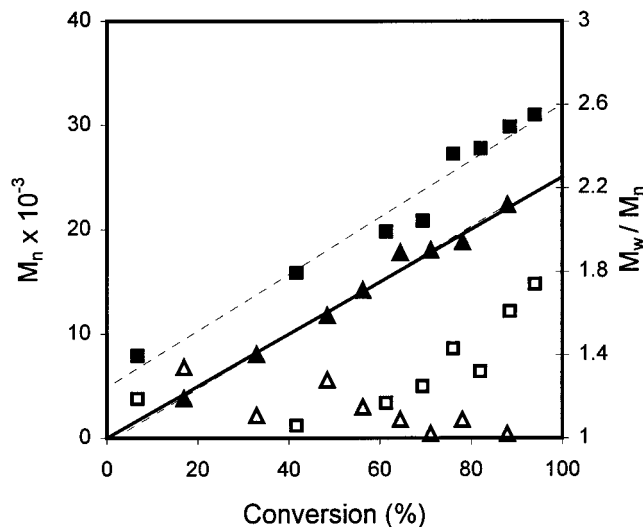


**Figure 6.** Number-average molecular weight versus percent conversion plot for the polymerization of MMA at 80 °C in anisole promoted by catalysts with noncoordinating tetraphenyl borate counterions,  $[\text{Cu}\{\text{en}(\text{Bn})\text{py}\}\text{Br}]\text{BPh}_4$  (■) and  $[\text{Cu}\{\text{en}(\text{Bn})\text{py}\}\text{Cl}]\text{BPh}_4$  (▲). (— =  $M_n(\text{calcd})$ ; corresponding open symbols represent PDIs).

comparable to reactions run with  $\text{Cu}\{\text{en}(\text{Bn})\text{py}\}\text{Br}$  under similar reaction conditions in the respective solvents (and presumably would be faster than for  $\text{Cu}\{\text{en}(\text{Bn})\text{py}\}\text{Cl}$ , though this catalyst was not tested). In addition, narrow molecular weight distributions ( $\text{PDI} < 1.1$ ) and excellent correlation between  $M_n$  and  $M_n(\text{calcd})$  values were noted (Figure 6). Halide exchange between the bromide initiator and less reactive chloride catalyst may be responsible for improved control in MMA polymerization. The chloride complex of the bulkier  $R,R$ -cn backbone ligand,  $[\text{Cu}\{R,R\text{-cn}(\text{F}_5\text{Bn})\text{py}\}\text{Cl}]\text{BPh}_4$ , also initiated MMA polymerization in toluene with an induction period of  $\sim 10$  min and complete monomer conversion in less than 2 h. Compared to reactions with the en backbone ligand, these systems show poor molecular weight control; molecular weights rapidly reached a plateau value of  $M_n = \sim 26\,000$ , and broader PDIs ( $\sim 1.4$ ) were observed throughout the course of the reaction.

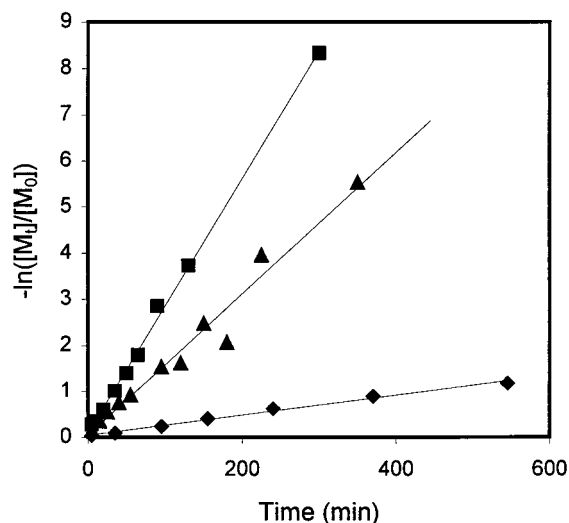


**Figure 7.** Kinetics plots for the polymerization of MMA in anisole at 80 °C employing catalysts with varying backbone and electronics,  $\text{Cu}\{\text{en}(\text{Bn})\text{py}\}\text{Br}$  (■),  $\text{Cu}\{R,R\text{-cn}(\text{Bn})\text{py}\}\text{Br}$  (▲), and the fluorinated  $\text{Cu}\{R,R\text{-cn}(\text{F}_5\text{Bn})\text{py}\}\text{Br}$  (◆), generated in situ.

In addition to varying metal oxidation states, halide ancillary ligands, and inner- and outer-sphere counterions, the electronic nature of copper catalysts was also modified by the introduction of fluorine substituents on the quadridentate ligands themselves. The en( $\text{F}_5\text{Bn}$ )py, **2**,  $R,R$ -cn( $\text{F}_5\text{Bn}$ )py, **6**, and  $R,R$ -cn( $\text{F}_5\text{Bn}$ )qn, **9**, chelates were combined with CuBr to generate  $\text{Cu}\{\text{en}(\text{F}_5\text{Bn})\text{py}\}\text{Br}$ ,  $\text{Cu}\{R,R\text{-cn}(\text{F}_5\text{Bn})\text{py}\}\text{Br}$ , and  $\text{Cu}\{R,R\text{-cn}(\text{F}_5\text{Bn})\text{qn}\}\text{Br}$  in situ in anisole and as preformed catalysts for reactions run in toluene. Polymerizations were slower and much more sensitive to reaction conditions when electron-withdrawing fluorinated ligands were present. Anisole reactions with en backbone ligands with and without fluorination exhibited good molecular weight control. Kinetics were first-order with respect to monomer (Figure 7). Reactions with en( $\text{F}_5\text{Bn}$ )py exhibited slightly slower rates ( $k_{\text{obs}} = 0.026\text{ min}^{-1}$ ) than those for en(Bn)py ( $k_{\text{obs}} = 0.028\text{ min}^{-1}$ ), as is expected for a more electron-deficient metal center that is harder to oxidize to Cu(II). The less reactive catalyst gives rise to slightly more controlled polymerization. Calculated molecular weights based on  $[\text{M}]_0/[\text{I}]_0$  show slightly better correlation with experiment for the fluorinated ligand; however, PDIs are comparable to those for polymers made from en(Bn)py (Figure 8). In both cases,  $M_n$  vs percent monomer conversion plots are linear. For the  $R,R$ -cn backbone ligand, however, more significant differences were observed between the catalysts with and without electron-withdrawing fluorine substituents on the chelating ligand. Again, the fluorinated ligands react more slowly, i.e., after  $\sim 1.5$  h, percent monomer conversion for  $R,R$ -cn(Bn)py: 78% ( $k_{\text{obs}} = 0.015\text{ min}^{-1}$ );  $R,R$ -cn( $\text{F}_5\text{Bn}$ )py: 21% ( $k_{\text{obs}} = 0.002\text{ min}^{-1}$ ). Molecular weight distributions for both systems remained narrow ( $< 1.2$ ) (Figure 9). For the bulkier quinoline analogues, **8** and **9**, poor molecular weight control was observed in both cases.

As for cyclohexyl backbone chelates, reactions employing preformed catalysts in toluene also displayed dramatic differences between fluorinated and nonfluorinated ligands. Again, though polymerizations with **1** and **5** proceeded smoothly, those with en( $\text{F}_5\text{Bn}$ )py, **2**,  $R,R$ -cn( $\text{F}_5\text{Bn}$ )py, **6**, and  $R,R$ -cn( $\text{F}_5\text{Bn}$ )qn, **9**, gave very low conversions in 10 h trial reactions (8%,  $\sim 6\%$ , and



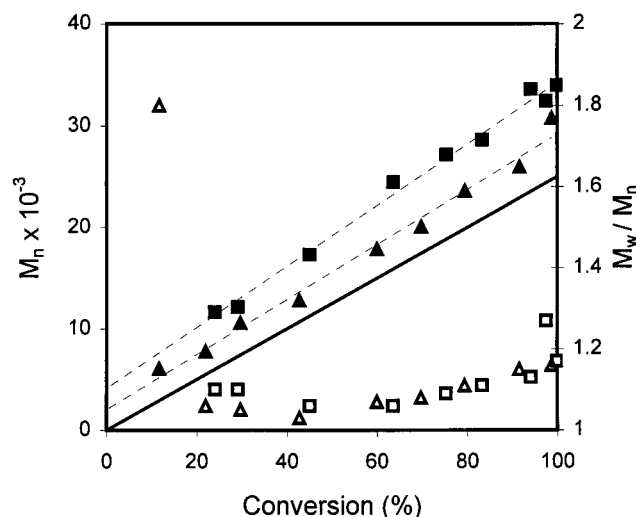


**Figure 8.** Comparison of  $M_n$  vs percent monomer conversion plots for the polymerization of MMA promoted by en backbone catalysts with different electronic features,  $\text{Cu}\{\text{en}(\text{Bn})\text{py}\}\text{Br}$  (■) and the fluorinated  $\text{Cu}\{\text{enF}_5(\text{Bn})\text{py}\}\text{Br}$  (▲), generated in situ at 80 °C in anisole. (— =  $M_n(\text{calcd})$ ; corresponding open symbols represent PDIs).

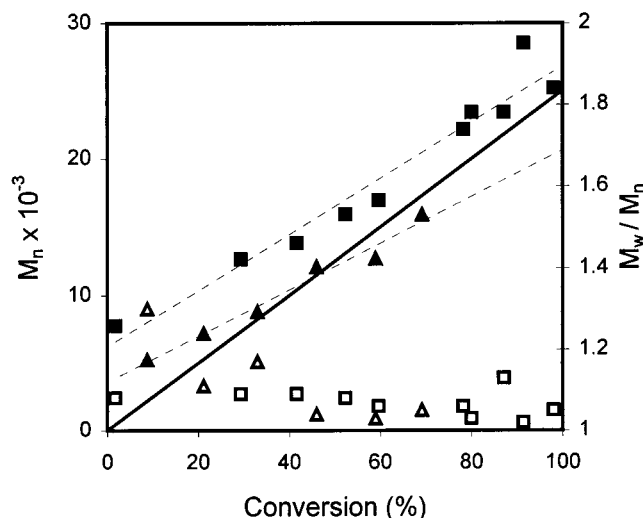


**Figure 9.** Comparison of  $M_n$  vs percent monomer conversion plots for the polymerization of MMA promoted by  $R,R$ -cn backbone catalysts with different electronic features,  $\text{Cu}\{R,R\text{-cn}(\text{Bn})\text{py}\}\text{Br}$  (■) and the fluorinated  $\text{Cu}\{R,R\text{-cnF}_5(\text{Bn})\text{py}\}\text{Br}$  (▲), generated in situ at 80 °C in anisole. (— =  $M_n(\text{calcd})$ ; corresponding open symbols represent PDIs).

1%, respectively). Polymer products of reactions utilizing  $\text{Cu}\{R,R\text{-cn}(\text{F}_5\text{Bn})\text{py}\}\text{Br}$  exhibited narrow molecular weight distributions ( $\text{PDI} \sim 1.16$ ), which suggests that this more electron-deficient catalyst might simply have an exceedingly long induction period.<sup>41</sup> However, GPC analysis of trace amounts of polymer isolated upon workup of 10 h reactions employing  $\text{Cu}\{R,R\text{-cn}(\text{F}_5\text{Bn})\text{qn}\}\text{Br}$  revealed that molecular weight control was poor as evidenced by a multimodal GPC trace. Trial reactions were also run with complexes bearing both fluorinated ligands and noncoordinating counterions. While comparable reaction rates and reasonable molecular weight control were observed for the en(Bn)py systems,  $\text{Cu}\{\text{en}(\text{Bn})\text{py}\}\text{Br}$  and  $[\text{Cu}\{\text{en}(\text{Bn})\text{py}\}\text{Cl}]\text{BPh}_4$ , reaction rates and molecular weight control differs considerably for  $\text{Cu}\{R,R\text{-cn}(\text{F}_5\text{Bn})\text{py}\}\text{Br}$  and  $[\text{Cu}\{R,R\text{-cn}(\text{F}_5\text{Bn})\text{py}\}\text{Cl}]\text{BPh}_4$ . Again, the  $\text{CuBr}/\mathbf{6}$  catalyst exhibited slow rates and low monomer conversion but good control, whereas

the  $\text{CuCl}-\text{BPh}_4/\mathbf{6}$  catalyst promoted complete monomer conversion in <2 h but with poor control. Molecular weights reached a plateau value,<sup>2</sup> and PDIs were broad throughout the reaction. Finally, reactions run with the sparingly soluble  $[\text{Cu}(\text{en}(\text{F}_5\text{Bn})\text{py})](\text{PF}_6)_2$  catalyst gave rise to ~8% conversion after 10 h, but once again molecular weight control was poor ( $\text{PDI} \sim 1.67$ ). Thus, preformed complexes with fluorinated chelates presented here are no longer viable catalysts for the controlled polymerization of MMA in toluene solution due to either slow reaction rates or poor molecular weight control as compared with their nonfluorinated counterparts. In summary, the introduction of electron-withdrawing groups onto the chelating ligands often influences MMA polymerization in a dramatic way, particularly in less polar toluene, further supporting the importance of electronic factors (i.e., metal oxidation potentials) on ATRP reactivity, as previously noted by Matyjaszewski.<sup>18,25</sup>

To investigate how steric features of the ligands affect reactivity of Cu catalysts, quadridentates were varied both in the diamine backbone and at the terminal donor positions. The influence of the ligand backbone was explored through the comparison of the reactivities of en and  $R,R$ -cn systems. Narrow molecular weight distributions ( $\text{PDI} < 1.2$ ) and linear  $M_n$  vs percent conversion plots were observed for Cu catalysts of both **1** and **2** and **5** and **6** pairs, shown in Figures 8 and 9, respectively. In anisole, the  $R,R$ -cn ligands show slower rates of reaction than en ligands (Figure 7); however, in toluene, this trend is reversed. In some respects, it is surprising that backbone substitution remote from the reaction center influences reactivity in such measurable ways. However, in addition to changing the electronic nature of the complex, the  $R,R$ -cn ligand is bulkier and more rigid. This may restrict conformational degrees of freedom and influence interactions between the nonchelating alkyl substituents,  $-\text{Bn}$  or  $-\text{F}_5\text{Bn}$ , and the reactive center. Prior  $^1\text{H}$  and  $^{13}\text{C}$  NMR studies on diamagnetic  $\text{Zn}(\text{II})$  complexes of these quadridentate chelates have indicated that subtle variations in the ligand backbone (en to methyl-substituted  $S$ -pn or  $R,R$ -cn) can often lead to differences in metal coordination number and geometry. Bulkier  $R,R$ -cn systems are more likely to dissociate halide ligands from their inner spheres to adopt lower coordinate structures.<sup>24</sup> Faster reaction rates for Cu  $R,R$ -cn systems vs en ones suggest that similar dissociative phenomena could be occurring with the copper series in toluene. This hypothesis gains further support from the fact that catalysts with non-coordinating counterions and, thus, lower coordination numbers also tend to be more reactive. However, the fact that the rate trend is reversed in anisole, a more polar solvent, runs counter to this argument. Catalyst solubility and the extent to which the various precomplexed Cu catalysts are oxidized to  $\text{Cu}(\text{II})$  could also be playing a role in the observed trends.

Steric effects were also explored through variation of the terminal donor groups of the quadridentate, from pyridine, to methylpyridine, and quinoline. In the en series, slightly increased rates were observed for catalysts with bulky quinoline groups, en(Bn)qn, **4**, versus the less hindered ligand, en(Bn)py, **1**. However, kinetics plots show a steady upward curvature<sup>13</sup> and, thus, an increase in rate throughout the course of the reaction. The  $M_n$  vs percent monomer conversion plot and PDIs for reactions with  $\text{Cu}\{\text{en}(\text{Bn})\text{qn}\}\text{Br}$  are also not consis-

**Table 2. Comparison of Fractions of Diads and Persistence Ratios of PMMA Generated from Selected Copper Catalysts**

catalyst	stereochemistry <sup>a</sup>					$\rho$
	mm	mr	rr	m	r	
Cu( <b>1</b> )Br	0.0221	0.312	0.666	0.178	0.822	0.938
Cu( <b>4</b> )Br	0.0256	0.340	0.635	0.195	0.805	0.924
Cu( <b>5</b> )Br	0.0267	0.339	0.635	0.196	0.804	0.931

<sup>a</sup> mm = isotactic triads; mr = atactic triads; rr = syndiotactic triads; m = meso diads; r = racemic diads;  $\rho$  = persistence ratio = 2(m)(r)/(mr).

tent with controlled polymerizations. In contrast, en catalysts prepared from 6-methylpyridine ligands **3** and **7** as well as the *R,R*-cn(Bn)qn system, **8**, all showed negligible reactivity<sup>41</sup> after 10 h. Others have made similar observations, in which too much steric bulk at the metal centers makes them less accessible for reaction with initiating and propagating centers, thus hindering halide abstraction.<sup>18</sup> Though the overall steric bulk of quinoline ligands **4** and **8** would seem to be greater than that of methylpyridines **3** and **7**, the sp<sup>2</sup> hybridized quinoline ring could exert very different steric demand on the reactive center as compared with an sp<sup>3</sup> methyl substituent in this position. It should also be noted that, for other metal ions, quite different geometries and ligand topologies have been observed with quinoline ligands relative to their pyridine analogues, due to the fact that it is not possible to accommodate bulky groups in planar structures.<sup>38</sup> We speculate that this might also account for the observed differences in reactivity.

**Polymer Microstructure.** Polymers synthesized in toluene using precomplexed Cu(L)Br (L = **1**, **4**, **5**) were subjected to <sup>13</sup>C NMR analysis to determine main chain tacticity from the backbone quaternary carbons (triad region, 44–46 ppm) according to the assignments proposed by Peat and Reynolds.<sup>44</sup> Triad fractions, diad fractions, and persistence ratios,  $\rho$ , for the PMMA backbones are listed in Table 2. These data are most consistent with Bernoullian statistics in which tacticity is dependent upon the last unit of the growing chain end only.<sup>45</sup> Ratios did not vary appreciably with increased sterics in either the ligand backbone (**1** vs **5**) or at the apical donor groups on the tertiary amine ligand (**1** vs **4**).<sup>36,46</sup> The lack of stereochemical control implies diffusion of the radical species away from the transition metal center prior to subsequent monomer addition. These results further confirm that chiral ATRP catalysts have little or no influence on polymer microstructure for simple monomers such as MMA and thus lend further support to the generally accepted mechanism of ATRP.<sup>1</sup>

## Conclusion

In summary, variation of steric and electronic features of quadridentate ligands bearing amine and pyridine donor groups leads to differences in ATRP catalyst reactivity. Moreover, reactions starting from CuBr and CuBr<sub>2</sub> salts of a given ligand produce polymer products with similar molecular weight control; however, catalysts generated from CuBr salts tend to react at faster rates. Reactions with catalysts generated in situ in anisole are generally faster and more controlled than comparable or precomplexed catalysts run in toluene. This could be due to enhanced solubility, to the fact that oxidation to Cu(II) is facilitated in the more polar

solvent, or to a combination of other factors that influence ATRP reaction rates and control. Abstraction of halides and replacement with noncoordinating BPh<sub>4</sub><sup>−</sup> counterions leads to even more reactive systems, analogous to what has been previously observed for Cu bpy catalysts. Improvements in reaction rates sometimes correlate with diminished molecular weight control. However, for BPh<sub>4</sub><sup>−</sup> salts of the en(Bn)py ligand this was addressed by a halide exchange strategy,<sup>19</sup> thus giving rise to the optimal quadridentate catalyst explored in this study. Polymerizations with [Cu{en(Bn)py}Cl]BPh<sub>4</sub> displayed good initiation, strong correlation between measured and calculated molecular weights, narrow molecular weight distributions, and reasonable rates of reaction. Dicationic PF<sub>6</sub><sup>−</sup> salts, in contrast, suffer from poor solubility in toluene and anisole solutions and thus are not effective catalysts for the ATRP of MMA under these conditions. The less electron-rich ligands bearing fluorine substituents are less reactive than nonfluorinated analogues, most significantly so in toluene solution, wherein molecular weight control is typically poor.

This study was limited to the polymerization of MMA using Cu catalysts and specific reaction conditions (i.e., temperature, loading, solvents). Further modification of reaction parameters could lead to enhanced reaction rates and molecular weight control. For MMA, it would be important to further address the issue of poor initiation in future studies. The excellent control observed with [Cu{en(Bn)py}Cl]BPh<sub>4</sub> in anisole suggests that bromide initiators coupled with CuCl in place of CuBr for in situ catalyst generation might be promising. Further modification of chelates, namely with electron-rich donating substituents,<sup>18</sup> could also lead to increased reaction rates while still maintaining acceptable molecular weight control. The potential of other metal quadridentate complexes to serve as ATRP catalysts could be further investigated,<sup>47</sup> and it also remains to apply this series of catalysts to the ATRP of other monomers and initiators under various reaction conditions. The results reported herein clearly demonstrate that copper complexes of picolylamine chelates are well-suited for systematic ATRP catalyst tuning. This family of ligands shows great promise for further application in atom transfer radical polymerization as well as other areas of chemistry.

## Experimental Section

**Materials.** Ligands en(Bn)py, **1**, en(F<sub>5</sub>Bn)py, **2**, en(Bn)qn, **4**, *R,R*-cn(Bn)py, **5**, *R,R*-cn(F<sub>5</sub>Bn)py, **6**, *R,R*-cn(Bn)pyMe, **7**, *R,R*-cn(Bn)qn, **8**, and *R,R*-cn(F<sub>5</sub>Bn)qn, **9**, and [Cu{*R,R*-cn(F<sub>5</sub>Bn)py}(PF<sub>6</sub>)<sub>2</sub>] were prepared as previously described.<sup>23,24,28</sup> Ethyl 2-bromoisobutyrate (98%), CuBr (minimum 98%), and CuBr<sub>2</sub> (99.999%) were obtained from Aldrich. Copper metal (powder) was purchased from Fisher. All other reagents and solvents were used as received.

**Instrumentation.** Polymers were characterized by GPC in CHCl<sub>3</sub> using a Hewlett-Packard 1100 system equipped with a vacuum degasser, a diode array detector, with a Polymer Labs "mixed c" guard column and two GPC columns, and with Wyatt Technology Corp. (WTC) DAWN multiangle laser light scattering (MALLS) and Optilab refractive index detectors and accompanying WTC Astra software. Unless otherwise indicated, a dn/dc value of 0.059 mL/g (PMMA in CHCl<sub>3</sub>) was used for MALLS molecular weight determination.<sup>48</sup> <sup>1</sup>H NMR and <sup>13</sup>C NMR spectra were recorded using a GE QE 300 spectrometer. Electronic absorption spectra were recorded on a Hewlett-Packard 8453 or 8452A diode array spectrophotometer in CH<sub>2</sub>Cl<sub>2</sub> or CH<sub>3</sub>CN solution. Cyclic voltammetric measurements



were made at room temperature with a Bioanalytical Systems model CV-50W instrument on dichloromethane solutions that contained 0.1 M tetra-*n*-butylammonium hexafluorophosphate (TBAH) as the supporting electrolyte at scan rates of 50 and 100 mV/s. Either a glassy carbon or a platinum working electrode in conjunction with a Pt-wire auxiliary electrode were utilized. Potentials were referenced to the aqueous Ag/AgCl electrode or the nonaqueous (CH<sub>3</sub>CN) Ag/AgNO<sub>3</sub> electrode. Elemental microanalyses were performed on a Perkin-Elmer model 2400 series II CHNS/O analyzer.

**en(Bn)pyMe, 3.** The en(Bn)pyMe ligand was synthesized by the procedure described previously for en(Bn)py with the following exceptions.<sup>23</sup> 6-Methyl-2-pyridinecarboxaldehyde was used instead of 2-pyridinecarboxaldehyde for the Schiff base synthesis. The Schiff base was obtained as a pale off-white solid. Yield: 1.21 g (95%). The secondary diamine was obtained as a white solid. Yield: 0.740 g (60%). After alkylation, in the final step of the workup, the tertiary diamine product precipitated from the acidic aqueous solution upon addition of the NaOH solution. The resultant white solid was collected and washed with additional H<sub>2</sub>O and EtOAc. Yield: 0.378 g (31%). <sup>1</sup>H NMR (300 MHz, CDCl<sub>3</sub>):  $\delta$  2.50 (s, 6H), 2.67 (s, 4H), 3.57 (s, 4H), 3.69 (s, 4H), 6.96 (d, *J* = 7.3 Hz, 2H), 7.20–7.31 (br m, 12H), 7.46 (t, *J* = 7.7 Hz, 2H).

**Preparation of Metal Complexes.** Copper(I) complexes were prepared by addition of EtOH solutions of CuBr to CH<sub>2</sub>Cl<sub>2</sub>/EtOH solutions of the free ligands. For the quinoline ligands **4**, **8**, and **9**, reaction solutions were refluxed for 30 min to facilitate dissolution of metal salt and ligand. Unless otherwise indicated, the CuBr was used as received. Room-temperature solutions were concentrated via rotary evaporation. The resultant residues were dissolved in a minimal amount of CH<sub>2</sub>Cl<sub>2</sub>, were filtered through glass wool, and were precipitated from rapidly stirring Et<sub>2</sub>O. Solids were collected by filtration, were washed with Et<sub>2</sub>O, and then were dried in vacuo. Deviations from these general procedures are indicated below for the respective compounds.

**Cu{en(Bn)py}Br.** CuBr (0.111 g, 0.770 mmol) was suspended in EtOH (2 mL) and then was added to an EtOH solution (3 mL) of en(Bn)py, **1** (0.325 g, 0.769 mmol). The green solution was concentrated via rotary evaporation and purified by the standard procedure to give a lime green powder. Yield: 0.172 g (63%).  $\Lambda_M = 89 \Omega^{-1} \text{ mol}^{-1} \text{ cm}^2$ .

**Cu{en(Bn)py}Br from Purified CuBr.** CuBr was purified as reported by Keller et al.<sup>49</sup> for reaction with **1** by the standard procedure to give a pale green powder. Yield: 0.098 g (33%).

**Cu{en(Bn)py}Br<sub>2</sub>·1/2CH<sub>2</sub>Cl<sub>2</sub>·1/2CH<sub>3</sub>CH<sub>2</sub>OH.** This complex was purified by recrystallization from EtOH/Et<sub>2</sub>O and was obtained as aqua needles after preparation by the general procedure. Yield: 0.281 g (84%).  $\Lambda_M = 116 \Omega^{-1} \text{ mol}^{-1} \text{ cm}^2$ . UV/vis [CH<sub>3</sub>CN,  $\lambda$  (nm),  $\epsilon_{\text{max}}$  (M<sup>-1</sup> cm<sup>-1</sup>): 262 (12 000), 302 (5800), 777 (320). Anal. Calcd for C<sub>29</sub>H<sub>33</sub>N<sub>4</sub>O<sub>0.5</sub>ClCuP<sub>2</sub>F<sub>12</sub>: C, 49.80; H, 4.82; N, 7.88. Found: C, 49.94; H, 5.22; N, 8.18.

**Cu{en(F<sub>5</sub>Bn)py}Br.** Pale green solid. Yield: 0.119 g (51%).  $\Lambda_M = 69 \Omega^{-1} \text{ mol}^{-1} \text{ cm}^2$ .

**Cu{en(Bn)pyMe}Br.** Lime green powder. Yield: 0.298 g (61%).  $\Lambda_M = 92 \Omega^{-1} \text{ mol}^{-1} \text{ cm}^2$ .

**Cu{en(Bn)qn}Br.** Mustard yellow powder. Yield: 0.183 g (65%).  $\Lambda_M = 82 \Omega^{-1} \text{ mol}^{-1} \text{ cm}^2$ .

**[Cu{en(Bn)py}][PF<sub>6</sub>]<sub>2</sub>.** CuCl<sub>2</sub>·2H<sub>2</sub>O (83.3 mg, 0.489 mmol) and en(Bn)py, **1**, (0.206 g, 0.488 mmol) were refluxed in CH<sub>3</sub>CN (1 mL) for 3 h. The blue solution was then cooled to room temperature (RT), and AgPF<sub>6</sub>(s) (0.247 g, 0.976 mmol) was added. After stirring for 30 min, the solution was filtered through a frit to remove a white precipitate. The resulting bright blue solution was concentrated via rotary evaporation. The blue residue was recrystallized from CH<sub>2</sub>Cl<sub>2</sub>/MeOH to give blue needles. Yield: 0.238 g (63%).  $\Lambda_M = 236 \Omega^{-1} \text{ mol}^{-1} \text{ cm}^2$ . UV/vis [CH<sub>3</sub>CN,  $\lambda$  (nm),  $\epsilon_{\text{max}}$  (M<sup>-1</sup> cm<sup>-1</sup>): 261 (13 000), 295 (6000), 632 (340).

**[Cu{en(Bn)py}Cl](BPh<sub>4</sub>)·CH<sub>3</sub>OH.** CuCl<sub>2</sub>·2H<sub>2</sub>O (0.116 g, 0.680 mmol) and **1** (0.223 g, 0.668 mmol) were refluxed in CH<sub>3</sub>CN (2 mL) for 1 h. The green solution was then allowed to cool to RT prior to addition of a CH<sub>3</sub>CN solution (1.3 mL) of NaBPh<sub>4</sub> (0.469 g, 1.37 mmol). A blue solid immediately

precipitated from the solution, and the resulting blue suspension was stirred for ~30 min. The pale blue powder was collected by filtration, was washed with additional CH<sub>3</sub>CN, and then was dissolved through the frit with CH<sub>2</sub>Cl<sub>2</sub> to remove a white solid. The blue filtrate was concentrated, and the residue was recrystallized from CH<sub>2</sub>Cl<sub>2</sub>/MeOH to give green needles. Yield: 0.391 g (67%).  $\Lambda_M = 79 \Omega^{-1} \text{ mol}^{-1} \text{ cm}^2$ . UV/vis [CH<sub>3</sub>CN,  $\lambda$  (nm),  $\epsilon_{\text{max}}$  (M<sup>-1</sup> cm<sup>-1</sup>): 260 sh, 293 sh, 762 (220). Anal. Calcd for C<sub>53</sub>H<sub>54</sub>N<sub>4</sub>OClBCu: C, 72.93; H, 6.24; N, 6.42. Found: C, 72.67; H, 6.24; N, 6.48.

**[Cu{en(Bn)py}Br](BPh<sub>4</sub>)·CH<sub>3</sub>OH.** This compound was synthesized as described above for [Cu{en(Bn)py}Cl](BPh<sub>4</sub>) except that CuBr<sub>2</sub> was used instead of CuCl<sub>2</sub>. The product was recrystallized from CH<sub>2</sub>Cl<sub>2</sub>/MeOH to give green needles. Yield: 0.169 g (72%).  $\Lambda_M = 82 \Omega^{-1} \text{ mol}^{-1} \text{ cm}^2$ . UV/vis [CH<sub>3</sub>CN,  $\lambda$  (nm),  $\epsilon_{\text{max}}$  (M<sup>-1</sup> cm<sup>-1</sup>): 260 sh, 290 sh, 777 (200). Anal. Calcd for C<sub>53</sub>H<sub>54</sub>N<sub>4</sub>OBrBCu: C, 69.40; H, 5.93; N, 6.11. Found: C, 68.91; H, 6.07; N, 6.12.

**Cu{R,R-cn(Bn)py}Br.** Mint green powder. Yield: 0.061 g (77%).  $\Lambda_M = 98 \Omega^{-1} \text{ mol}^{-1} \text{ cm}^2$ . UV/vis [CH<sub>3</sub>CN,  $\lambda$  (nm),  $\epsilon_{\text{max}}$  (M<sup>-1</sup> cm<sup>-1</sup>): 262 (9900), 311 (5600), 730 (250).

**Cu{R,R-cn(Bn)py}Br<sub>2</sub>·1/2CH<sub>2</sub>Cl<sub>2</sub>·1/2CH<sub>3</sub>CH<sub>2</sub>OH.** The Cu(II) catalyst was synthesized as above for Cu{R,R-cn(Bn)py}Br except that CuBr<sub>2</sub> was used instead of CuBr. The product was obtained as a pale green powder. Yield: 0.095 g (73%).  $\Lambda_M = 120 \Omega^{-1} \text{ mol}^{-1} \text{ cm}^2$ . Anal. Calcd for C<sub>33.5</sub>H<sub>40</sub>N<sub>4</sub>O<sub>0.5</sub>ClBr<sub>2</sub>·Cu: C, 52.56; H, 5.27; N, 7.32. Found: C, 52.42; H, 5.72; N, 7.40.

**Cu{R,R-cn(F<sub>5</sub>Bn)py}Br.** Lime green powder. Yield: 0.116 g (37%).  $\Lambda_M = 96 \Omega^{-1} \text{ mol}^{-1} \text{ cm}^2$ .

**Cu{R,R-cn(Bn)pyMe}Br.** Pale yellow-green powder. Yield: 0.146 g (58%).  $\Lambda_M = 97 \Omega^{-1} \text{ mol}^{-1} \text{ cm}^2$ .

**Cu{R,R-cn(Bn)qn}Br.** Yellow-orange powder. Yield: 0.087 g (60%).  $\Lambda_M = 99 \Omega^{-1} \text{ mol}^{-1} \text{ cm}^2$ .

**Cu{R,R-cn(F<sub>5</sub>Bn)qn}Br·CH<sub>2</sub>Cl<sub>2</sub>·CH<sub>3</sub>CH<sub>2</sub>OH.**<sup>50</sup> This compound was recrystallized from MeOH/Et<sub>2</sub>O to give yellow needles. Yield: 0.134 g (73%).  $\Lambda_M = 113 \Omega^{-1} \text{ mol}^{-1} \text{ cm}^2$ . <sup>1</sup>H NMR (CDCl<sub>3</sub>, 300 MHz):  $\delta$  1.49 (1.45–1.52) (m, 2H), 1.70 (1.64–1.75) (m, 2H), 2.02 (2.00–2.04) (m, 2H), 2.55 (2.52–2.57) (m, 2H), 4.06 (d, *J* = 13.5 Hz, 2H), 4.34 (4.28–4.40) (m, 6H), 7.56 (7.54–7.59) (m, 2H), 7.66 (7.63–7.68) (m, 2H), 7.79 (7.75–7.82) (m, 4H), 7.98 (d, *J* = 7.3 Hz, 2H), 8.42 (d, *J* = 7.7 Hz, 2H). UV/vis [CH<sub>3</sub>CN,  $\lambda$  (nm),  $\epsilon_{\text{max}}$  (M<sup>-1</sup> cm<sup>-1</sup>): 285 sh, 309 (9600), 321 (9800), 395 (2700). Anal. Calcd for C<sub>43</sub>H<sub>38</sub>N<sub>4</sub>O<sub>10</sub>Cl<sub>2</sub>BrCu: C, 50.09; H, 3.71; N, 5.43. Found: C, 50.59; H, 3.90; N, 5.65.

**[Cu{R,R-cn(F<sub>5</sub>Bn)py}Cl](BPh<sub>4</sub>).** This compound was synthesized as described above for [Cu{en(Bn)py}Cl](BPh<sub>4</sub>) except that R,R-cn(F<sub>5</sub>Bn)py, **6**, was used instead of **1**. Pale lime-green solid. Yield: 0.278 g (63%).  $\Lambda_M = 96 \Omega^{-1} \text{ mol}^{-1} \text{ cm}^2$ . UV/vis [CH<sub>3</sub>CN,  $\lambda$  (nm),  $\epsilon_{\text{max}}$  (M<sup>-1</sup> cm<sup>-1</sup>): 260 sh, 273 sh, 286 sh, 351 (2700), 676 (39).

**Representative Procedures for *M<sub>n</sub>* vs Percent Conversion Studies.** *Reactions with preformed catalysts prepared from CuX:* Cu{R,R-cn(Bn)py}Br (0.058 g, 0.934 mmol) and copper metal (1.6 mg, 0.025 mmol) were added to a Schlenk tube. The system was subjected to three evacuation/nitrogen fill cycles. MMA (2.41 g, 24.1 mmol) followed by toluene (2.16 g, ~2.5 mL) and ethyl 2-bromoisobutyrate (0.019 g, 0.096 mmol) were added to the reaction vessel, which was subsequently sealed under nitrogen and heated in an 80 °C oil bath. After the designated times, aliquots (~0.5 mL) were removed, transferred to small, tarred round-bottom flasks, and rapidly cooled in an ice water bath. All volatiles were removed in vacuo, and percent conversion was determined by gravimetric analysis. Molecular weight analysis was conducted prior to purification. *Reactions with preformed Cu(II) catalysts:* Reactions were run as above, but 1 equiv of Cu(0) was used per equivalent of Cu catalyst. *Reactions with catalysts formed in situ:* In situ polymerizations were conducted in an analogous manner except that the CuBr and the appropriate ligand were added to the Schlenk tube, and no Cu(0) was added. Reagent loadings: initiator/CuBr/ligand/MMA = 1/1/1.5/250; 1:1 MMA: solvent (v/v) (solvent = anisole or toluene).

**General Procedure for Preparative Reactions for Determination of Polymer Tacticity.** Preparative reactions were performed as described above with the following exceptions. After cooling, reaction mixtures were dissolved in  $\text{CH}_2\text{Cl}_2$  and were transferred to a round-bottom flask for concentration via rotary evaporation. The resultant residues were purified by passage of THF solutions through basic alumina, followed by precipitation from THF/heptanes (2 times). After collection by filtration, the polymer samples were dried in vacuo for  $\sim 1$  d to give white powdery solids. Typical yield:  $\sim 50\%$ .

**Acknowledgment.** We gratefully acknowledge Dupont for a Young Professor Grant and the University of Virginia for support for this work.

## References and Notes

- (1) For recent reviews on ATRP see: (a) Patten, T. E.; Matyjaszewski, K. *Acc. Chem. Res.* **1999**, *32*, 895. (b) Matyjaszewski, K., Ed. *Controlled Radical Polymerizations*; ACS Symposium Series 685; American Chemical Society: Washington, DC, 1998. (c) Patten, T. E.; Matyjaszewski, K. *Adv. Mater.* **1998**, *10*, 901. (d) Sawamoto, M.; Kamigaito, M. *Trends Polym. Sci.* **1996**, *4*, 371. (e) Baumert, M.; Frey, H.; Holderle, M.; Kressler, J.; Sernetz, F. G.; Mulhaupt, R. *Macromol. Symp.* **1997**, *121*, 53.
- (2) Matyjaszewski, K.; Wang, J.-L.; Grimaud, T.; Shipp, D. A. *Macromolecules* **1998**, *31*, 1527.
- (3) (a) Ando, T.; Kamigaito, M.; Sawamoto, M. *Tetrahedron* **1997**, *53*, 15445. (b) Haddleton, D. M.; Heming, A. M.; Kukulj, D.; Duncalf, D. J.; Shooter, A. J. *Macromolecules* **1998**, *31*, 2016. (c) Percec, V.; Barboiu, B.; Kim, H.-J. *J. Am. Chem. Soc.* **1998**, *120*, 305 and references therein.
- (4) (a) Haddleton, D. M.; Duncalf, D. J.; Kukulj, D.; Radigue, A. P. *Macromolecules* **1999**, *32*, 4769. (b) Ando, T.; Kamigaito, M.; Sawamoto, M. *Macromolecules* **2000**, *33*, 2819. (c) Takashi, H.; Ando, T.; Kamigaito, M.; Sawamoto, M. *Macromolecules* **1999**, *32*, 6461.
- (5) Moineau, G.; Granel, C.; Dubois, Ph.; Jérôme, R.; Teyssié, P. *Macromolecules* **1998**, *31*, 542.
- (6) (a) Ando, T.; Kamigaito, M.; Sawamoto, M. *Macromolecules* **1997**, *30*, 4507. (b) Matyjaszewski, K.; Wei, M.; Xia, J.; McDermott, N. E. *Macromolecules* **1997**, *30*, 8161.
- (7) (a) Granel, C.; Dubois, P.; Jérôme, R.; Teyssié, P. *Macromolecules* **1996**, *29*, 8576. (b) Uegaki, H.; Kotani, Y.; Kamigaito, M.; Sawamoto, M. *Macromolecules* **1997**, *30*, 2249. (c) Uegaki, H.; Kotani, Y.; Kamigaito, M.; Sawamoto, M. *Macromolecules* **1998**, *31*, 6756. (d) Hawker, C. J.; Hedrick, J. L.; Malmström, E. E.; Trollsås, M.; Mecerreyes, D.; Moineau, G.; Dubois, Ph.; Jérôme, R. *Macromolecules* **1998**, *31*, 213.
- (8) Moineau, G.; Minet, M.; Dubois, Ph.; Teyssié, P.; Senninger, T.; Jérôme, R. *Macromolecules* **1999**, *32*, 27.
- (9) Kotani, Y.; Kamigaito, M.; Sawamoto, M. *Macromolecules* **1999**, *32*, 2420.
- (10) Matyjaszewski, K.; Patten, T. E.; Xia, J. *J. Am. Chem. Soc.* **1997**, *119*, 674 and references therein.
- (11) Wang, J.-L.; Grimaud, T.; Matyjaszewski, K. *Macromolecules* **1997**, *30*, 6507.
- (12) Arehart, S. V.; Matyjaszewski, K. *Macromolecules* **1999**, *32*, 2221.
- (13) Xia, J.; Matyjaszewski, K. *Macromolecules* **1997**, *30*, 7697.
- (14) (a) Xia, J.; Gaynor, S. G.; Matyjaszewski, K. *Macromolecules* **1998**, *31*, 5958. (b) Kikelbick, G.; Matyjaszewski, K. *Macromol. Rapid Commun.* **1999**, *20*, 341.
- (15) Xia, J.; Matyjaszewski, K. *Macromolecules* **1999**, *32*, 2434.
- (16) Haddleton, D. M.; Crossman, M. C.; Dana, B. H.; Duncalf, D. J.; Heming, A. H.; Kukulj, D.; Shooter, A. J. *Macromolecules* **1999**, *32*, 2110 and references therein.
- (17) (a) Haddleton, D. M.; Kukulj, D.; Duncalf, D. J.; Heming, A. M.; Shooter, A. J. *Macromolecules* **1998**, *31*, 5201. (b) Haddleton, D. M.; Jasieczek, C. B.; Hannon, M. J.; Shooter, A. J. *Macromolecules* **1997**, *30*, 2190. (c) Hovestad, N. J.; van Koten, G.; Bon, S. A. F.; Haddleton, D. M. *Macromolecules* **2000**, *33*, 4048.
- (18) Matyjaszewski, K.; Xia, J. H.; Zhang, X. *PMSE Prepr.* **1999**, *80*, 453.
- (19) (a) Matyjaszewski, K.; Shipp, D. A.; Wang, J.-L.; Grimaud, T.; Patten, T. E. *Macromolecules* **1998**, *31*, 6831. (b) Haddleton, D. M.; Heming, A. M.; Kukulj, D.; Jackson, S. G. *Chem. Commun.* **1998**, 1719. (c) Teodorescu, M.; Gaynor, S. G.; Matyjaszewski, K. *Macromolecules* **2000**, *33*, 2335.
- (20) Woodworth, B. E.; Metzner, Z.; Matyjaszewski, K. *Macromolecules* **1998**, *31*, 7999.
- (21) Matyjaszewski, K.; Wei, M.; Xia, J.; Gaynor, S. G. *Macromol. Chem. Phys.* **1998**, *199*, 2289.
- (22) Davis, K. A.; Paik, H.-J.; Matyjaszewski, K. *Macromolecules* **1999**, *32*, 1767 and references therein.
- (23) Ng, C.; Sabat, M.; Fraser, C. L. *Inorg. Chem.* **1999**, *38*, 5545.
- (24) Ng, C.; Savage, S. A.; Sabat, M.; Fraser, C. L. Unpublished results.
- (25) (a) Matyjaszewski, K. *Macromol. Symp.* **1998**, *134*, 105. (b) Matyjaszewski, K.; Woodworth, B. E. *Macromolecules* **1998**, *31*, 4718.
- (26) (a) Haddleton, D. M.; Duncalf, D. J.; Kukulj, D.; Crossman, M. C.; Jackson, S. G.; Bon, S. A. F.; Clark, A. J.; Shooter, A. J. *Eur. J. Inorg. Chem.* **1998**, 1799. (b) For another use of these ligands in radical reactions see: Clark, A. J.; Duncalf, D. J.; Filik, R. P.; Haddleton, D. M.; Thomas, G. H.; Wongtap, H. *Tetrahedron Lett.* **1999**, *40*, 3807.
- (27) Methylation of the internal  $2^\circ$  amine nitrogens may be achieved by reductive amination using formaldehyde and sodium cyanoborohydride.<sup>24</sup> Fenton, R. R.; Stephens, F. S.; Vagg, R. S.; Williams, P. A. *Inorg. Chim. Acta* **1991**, *182*, 67.
- (28) Rieger, B.; Abu-Surrah, A. S.; Fawzi, R.; Steiman, M. J. *Organomet. Chem.* **1995**, *497*, 73.
- (29) Gazo, J.; Bersuker, I. B.; Garaj, J.; Kabesova, M.; Kohout, J.; Langfelderova, H.; Melnyk, M.; Serator, M.; Valach, F. *Coord. Chem. Rev.* **1976**, *19*, 253.
- (30) (a) Hathaway, B. J. *J. Chem. Soc., Dalton Trans.* **1972**, 1196. (b) Hathaway, B. J.; Billing, D. E. *Coord. Chem. Rev.* **1970**, *5*, 143. (c) *Comprehensive Coordination Chemistry*; Wilkinson, G., Ed.; Pergamon Press: Oxford, 1987; Vol. 5, Chapter 53, pp 594–744. (d) Also see: Amundsen, A. R.; Whelan, J.; Bosnich, B. *J. Am. Chem. Soc.* **1977**, *99*, 6730.
- (31) (a) Gibson, J. G.; McKenzie, E. D. *J. Chem. Soc. (A)* **1971**, 1666 and references therein. (b) Bailey, N. A.; McKenzie, E. D.; Worthington, J. M. *J. Chem. Soc., Dalton Trans.* **1973**, 1227. (c) Pajunen, A.; Pajunen, S. *Acta Crystallogr.* **1986**, *C42*, 53. (d) McKenzie, E. D.; Stephens, F. S. *Inorg. Chim. Acta* **1980**, *42*, 1.
- (32) Goodwin, H. A.; Lions, F. *J. Am. Chem. Soc.* **1960**, *82*, 5013.
- (33) Nikles, D. E.; Powers, M. J.; Urbach, F. L. *Inorg. Chem.* **1983**, *22*, 3210.
- (34) Sakurai, T.; Kimura, M.; Nakahara, A. *Bull. Chem. Soc. Jpn.* **1981**, *54*, 2976.
- (35) *Comprehensive Coordination Chemistry*; Wilkinson, G., Ed.; Pergamon Press: Oxford, 1987; Vol. 5, Chapter 53, pp 535–593.
- (36) For an example of the use of a chiral Cu(I) catalyst in ATRP, see: Haddleton, D. M.; Duncalf, D. J.; Kukulj, D.; Heming, A. M.; Shooter, A. J.; Clark, A. J. *J. Mater. Chem.* **1998**, *8*, 1525.
- (37) Matyjaszewski, K.; Coca, S.; Gaynor, S. G.; Wei, M.; Woodworth, B. E. *Macromolecules* **1998**, *31*, 5967.
- (38) These steric effects, referred to as “B strain”, have been discussed by Gibson and McKenzie.<sup>31a</sup> Newkome and co-workers have observed a similar “obstacle effect” in Pd(II) complexes of picolylamines. Newkome, G. R.; Frere, Y. A.; Fronczek, F. R.; Gupta, V. K. *Inorg. Chem.* **1985**, *24*, 1001. See ref 32 for additional examples.
- (39) AgBPh<sub>4</sub> was prepared by a modification of previously reported preparations for AgBARf<sup>+</sup> and AgBPh<sub>4</sub>. Aqueous solutions of AgNO<sub>3</sub> were combined with various solutions of NaBPh<sub>4</sub> (Et<sub>2</sub>O, EtOH, acetone, or H<sub>2</sub>O) to yield white solid precipitates. These solids were either insoluble or sparingly soluble in a variety of media (Et<sub>2</sub>O, EtOH, MeOH, CH<sub>2</sub>Cl<sub>2</sub>, CH<sub>3</sub>CN, acetone) even at elevated temperatures. Beige and/or silver impurities formed in the solids over time ( $\sim 3$  days) even when stored under vacuum and protected from light. This is consistent with observations previously reported for this and related silver salts. (a) Hayashi, Y.; Rohde, J. J.; Corey, E. J. *J. Am. Chem. Soc.* **1996**, *118*, 5501. (b) Golden, J. H.; Mutolo, P. F.; Lobkovsky, E. B.; DiSalvo, F. J. *Inorg. Chem.* **1994**, *33*, 5374. (c) Popovych, O. *Anal. Chem.* **1966**, *38*, 117.
- (40) Haddleton, D. M.; Clark, A. J.; Crossman, M. C.; Duncalf, D. J.; Heming, A. M.; Morsley, S. R.; Shooter, A. J. *Chem. Commun.* **1997**, 1173.
- (41) Reactions that failed to show appreciable conversion ( $<10\%$ ) after 10 h trial reactions were considered to display negligible reactivity. It is possible, however, that some of these com-

- plexes are still effective catalysts for the ATRP of MMA but that they possess long induction periods or they react very slowly.
- (42) Since in situ reactions with purified CuBr, **5**, and xylenes in the absence of Cu(0) did proceed to an appreciable extent but with slightly broader molecular weight distributions (PDI  $\sim 1.3$ ), the lower reactivity is probably attributable to partial oxidation of Cu(I) during precomplexed catalyst preparation.
  - (43) Tetraphenyl borate salts have been used as photoinitiators in polymerization reactions. Popielarz, R.; Sarker, A. M.; Neckers, D. C. *Macromolecules* **1998**, *31*, 951. Dissociation of phenyl radicals from tetraphenyl borate counterions does not appear to be competitive under these reaction conditions. An increase in the initiator radical concentration could give rise to depressed  $M_n$  vs percent conversion plots relative to the calculated values. And since initiation from phenyl radicals thus formed is likely to differ from that of the  $\alpha$ -bromoester initiator, nonlinear first-order kinetics seem likely. In this study, polymerizations utilizing Cu catalysts with  $\text{BPh}_4^-$  counterions are faster but in other respects are often comparable to reactions without  $\text{BPh}_4^-$  present. Molecular weights tend to be greater, not less, than the calculated values, and kinetics plots are often linear.
  - (44) Peat, I. R.; Reynolds, W. F. *Tetrahedron Lett.* **1972**, *14*, 1359.
  - (45) Odian, G. *Principles of Polymerization*, 3rd ed.; John Wiley & Sons: New York, 1991; pp 675–80.
  - (46) Wang, J.-S.; Jérôme, R.; Warin, R.; Teyssié, P. *Macromolecules* **1993**, *26*, 5984.
  - (47) Preliminary studies have been conducted with  $\text{en}(\text{Bn})\text{py}$ , **1**, and other  $\text{MBr}_2$  salts ( $\text{M}(\text{II}) = \text{Fe}, \text{Co}, \text{Ni}, \text{Zn}$ ). Complexes were prepared analogous to copper catalyst synthesis and were purified by precipitation from  $\text{CH}_2\text{Cl}_2/\text{Et}_2\text{O}$  or by recrystallization using layering techniques and  $\text{EtOH}/\text{Et}_2\text{O}$ . Complexes were screened as catalysts for MMA polymerization in toluene solution at 80 °C using ethyl 2-bromoisobutyrate as the initiator. Zinc, cobalt, and iron complexes did not promote MMA polymerization ( $\sim 0\%$  conversion) after  $\sim 1$  day. The following could explain why these systems are poor catalysts for ATRP. For Zn(II), there exists no accessible higher oxidation state. Upon halide abstraction, a Co(II) complex would be converted to an inert Co(III)-Br species that is not likely to readily cycle back to the Co(II) oxidation state to cap the radical species that are generated. Iron complexes, for which both Fe(II) and Fe(III) oxidation states are accessible, could be more promising as ATRP catalysts. However, electronic tuning and/or the generation of an Fe(II) complex with a vacant coordination site rather than a coordinatively saturated octahedral structure may be required, along with optimization of other reaction parameters. In contrast to the poor reactivity of MMA in the presence of the aforementioned metals, the nickel complex,  $\text{Ni}\{\text{en}(\text{Bn})\text{py}\}\text{Br}_2$ , did catalyze polymerization of MMA, but molecular weights were high and molecular weight distributions were broad ( $\text{EtOH}/\text{Et}_2\text{O}$  purification:  $M_n = 83\,840$ , 48% conversion;  $\text{CH}_2\text{Cl}_2/\text{Et}_2\text{O}$  purification: 17, 260, 15% conversion; PDIs  $\sim 2.2$ –3.9).
  - (48) *Polymer Handbook*, 3rd ed.; Brandup, J., Immergut, E. H., Eds.; John Wiley and Sons: New York, 1989; p VII/430.
  - (49) Keller, R. N.; Wycoff, H. D. *Inorg. Synth.* **1947**, *2*, 1.
  - (50) The  $^1\text{H}$  NMR spectrum of this complex in  $\text{CDCl}_3$  supports the presence of 1 mol equiv of both  $\text{CH}_2\text{Cl}_2$  and  $\text{EtOH}$ .  
MA9911905